

## Formulation of Chemically Reduced Graphene Oxide Assembly with Poly(4-vinyl pyridine) Through Noncovalent Interaction

Mi Yeon Lee,<sup>1</sup> Su Hyun Nam,<sup>2,3</sup> Jung Yup Lee,<sup>1</sup> Abdullah-Al-Nahain,<sup>4</sup> Sangkug Lee,<sup>5</sup>  
Cheol Min Park,<sup>3</sup> Chul Jong Han,<sup>2</sup> Sung Young Park,<sup>4</sup> Insik In<sup>1</sup>

<sup>1</sup>Department of Polymer Science and Engineering, Korea National University of Transportation, Chungju, Chungbuk 380-702, Republic of Korea

<sup>2</sup>Flexible Display Research Center, Korea Electronics Technology Institute, Seongnam-Si, Gyeonggi-do, Republic of Korea

<sup>3</sup>Nano Polymer Laboratory, Yonsei University, 50 Yonsei-ro, Seodaemun-gu, Seoul, Republic of Korea

<sup>4</sup>Department of Chemical and Biological Engineering, Korea National University of Transportation, Chungju 380-702, Republic of Korea

<sup>5</sup>IT Convergence Material R&D Group, Korea Institute of Industrial Technology, Cheonan 330-825, Republic of Korea

Correspondence to: S. Y. Park (E-mail: parkchem@ut.ac.kr) or I. In (E-mail: in1@ut.ac.kr)

**ABSTRACT:** Soluble chemically reduced graphene oxide (RGO)/poly(4-vinyl pyridine) (P4VP) assembly was attempted by totally non-covalent approach. Chemical reduction of P4VP/GO mixture by hydrazine produced soluble RGO/P4VP assembly with long term stability. Prepared RGO/P4VP assembly showed pH-dependent variation of optical transmittance. Transmittance of RGO/P4VP assembly solution at pH 2.0 dramatically increased more than 200% of transmittance of assembly at pH 6. This optical transmittance change was fully reversible. The detailed morphological features of assemble was evaluated by dynamic light scattering (DLS) and atomic force microscopy (AFM). It is estimated that RGO/P4VP assemblies were well separated each other at pH 6, enabling much higher optical absorption of RGO plates. At pH 2, protonation of pyridine ring occurs and this might hamper effective noncovalent interaction between RGO plate and protonated P4VP chains, forming bigger aggregates having less chance for optical absorption. This pH-dependent optical modulation of RGO/P4VP assembly can be useful for the designing of pH-sensor, removable nanocatalyst, and targeted drug delivery, etc. © 2013 Wiley Periodicals, Inc. *J. Appl. Polym. Sci.* 130: 2538–2543, 2013

**KEYWORDS:** self-assembly; nanoparticles; nanowires and nanocrystals; nanostructured polymers; optical properties

Received 24 February 2013; accepted 24 April 2013; Published online 27 May 2013

DOI: 10.1002/app.39468

### INTRODUCTION

Two dimensional (2D) graphene has received intensive research interests due to its fascinating mechanical, thermal, electric, and optical properties.<sup>1,2</sup> Both “wet chemistry” using soluble graphene oxide (GO) or chemically reduced graphene oxide (RGO)<sup>3,4</sup> and “dry chemistry” such as chemical vapor deposition (CVD)<sup>5</sup> have been unveiled to prepare graphene-based nanomaterials or nanodevices. Among these, the idea of “soluble graphene” is one of the most promising approaches to fabricate graphene-based film in large area with much lower processing cost.<sup>6</sup>

To formulate soluble RGO in solvent media, certain functionalization of graphene plates by charges, small molecules, or polymers must be performed through either covalent<sup>7–11</sup> or noncovalent chemistry<sup>6</sup> because pristine graphene or RGO itself is not readily soluble in any solvent media due to its extremely

high van der Waals interaction (or van der Waals force) between 2D graphene plates. Among noncovalent chemistry,  $\pi$ - $\pi$  interaction is the most frequently attempted noncovalent interaction to formulate soluble RGO/ $\pi$ -conjugated polymer assembly.<sup>12,13</sup> While  $\sigma$ - $\pi$  interaction is typically much weaker than  $\pi$ - $\pi$  interaction, recent researches on noncovalent formulation of soluble RGO/polymer assembly have revealed that  $\sigma$ -rich aliphatic polymers can be noncovalently anchored on RGO plate.<sup>14–22</sup> From the fact that  $\sigma$ - $\pi$  interaction is enhanced in the presence of long polyene, significant  $\sigma$ - $\pi$  interaction between RGO plates and aliphatic polymers can be expected because graphene is a kind of conjugated 2D polyene.<sup>23</sup> Recent theoretical simulations for the anchoring of certain amino acid molecules or cholesterol on ideal graphene plates have revealed that aliphatic molecules with various molecular weights can be spontaneously anchored on graphene plates through van der Waals interaction.<sup>24,25</sup> But the detailed interaction parameter between RGO plates and

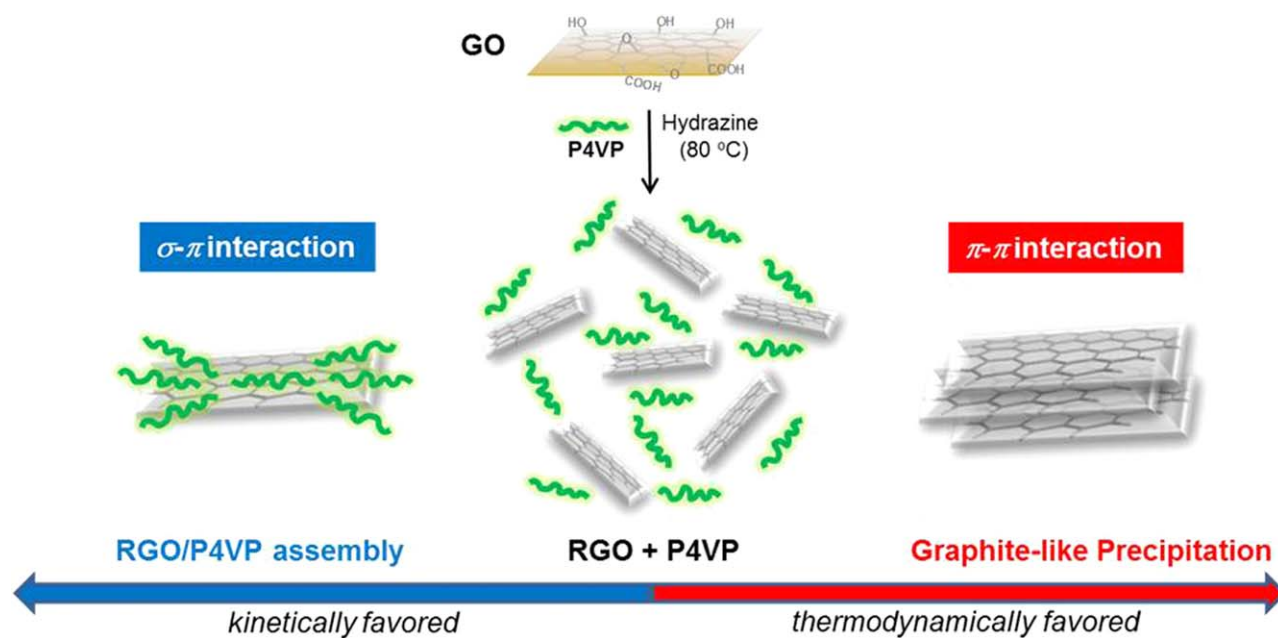


**Figure 1.** Schematic illustration for the formation of RGO/P4VP assembly through noncovalent interaction (two dominating interactions were compared with the obtained structures). [Color figure can be viewed in the online issue, which is available at [wileyonlinelibrary.com](http://wileyonlinelibrary.com).]

aliphatic polymers was not fully unveiled and therefore further theoretical and experimental researches to elucidate the feature of noncovalent interaction between RGO plates and aliphatic polymers are required.

Poly(4-vinyl pyridine) (P4VP), a simple water soluble polymer, is one of good molecular probes to examine interaction parameter and morphological feature of RGO/aliphatic polymer assembly. Especially, the positively chargeable pyridine groups of P4VP chains might provide significant change on the microenvironment of RGO/P4VP assembly. This change of microenvironment might induce significant variation on the morphological feature of assembly, enabling fine tuning of chemical, or physical properties of graphene. For example, optical property of RGO is strongly correlating with its dispersion state.<sup>26</sup> Well dispersed RGO solution shows higher optical absorbance in the same concentration of RGO because most RGO plates have chances for optical absorption in this case. Highly aggregated RGO plates might induce less optical absorbance because strong optical absorption of outer RGO plates can hamper optical absorption of inner RGO plates in aggregates.<sup>18</sup> In this study, RGO/P4VP assembly which shows fully reversible optical modulation through controlling of pH will be formulated. Optical modulation of resulting RGO/P4VP assembly in different pH will be correlated with the variation of morphological feature of RGO/P4VP assembly.

## EXPERIMENTAL

### Materials and Instruments

All chemicals were purchased from Sigma-Aldrich Corporation. Graphite powder (SP-1) was purchased from Bay Carbon Incorporated. P4VP having weight average molecular weight of 40,000 g/mol was used as received. Ultraviolet–Visible (UV–Vis) spectra were obtained from UV–Vis spectrometer of Hewlett Packard. Photoluminescence (PL) spectra were obtained from

L550B luminescence spectrometer of Perkin Elmer. Fourier transform Infrared (FT-IR) spectra were obtained from IR100/IR200 spectrometer of Thermolectron Corporation. Dynamic light scattering (DLS) data were obtained from particle size analyzer (ELS-Z) of Otsuka Electronics Corporation. Field emission-scanning electron microscope (FE-SEM) images were obtained from JSM-6700 field emission scanning electron microscope of GELO Corporation. Atomic force microscopy (AFM) images were obtained from XE-100 atomic force microscope of PSIA. Raman spectra were obtained from LabRAM high resolution dispersive Raman microscope of Horiba Jobin Yvon using a 633 nm He–Ne laser beam.

### Preparation of RGO/P4VP Assembly

GO was prepared from natural graphite by a modified Hummers method.<sup>27</sup> For experiments, fresh GO solution (1.00 mg of GO in 10 mL of deionized water) was prepared with minimum sonication (no more than 30 min below 10°C) just before use. Then, 10.0 mg of P4VP in 25 mL of 10 wt % aqueous acetic acid was simply magnetically mixed with GO solution, resulting in bright brown GO/P4VP mixture solution. To chemically reduce GO into RGO, four drops of hydrazine monohydrate (30 wt % aqueous solution) were added into above GO/P4VP mixture solution and the reaction temperature was maintained at 80°C for 24 h, producing dark black-colored RGO/P4VP assembly solution with optical clarity. Prepared RGO/P4VP assembly was stable for more than 6 months without any visible precipitation.

## RESULTS AND DISCUSSION

### Formation of Soluble RGO/P4VP Assembly

Formation of RGO/P4VP assembly was attempted through fully noncovalent approach as shown in Figure 1. All reactions were performed in the medium of aqueous acetic acid solution

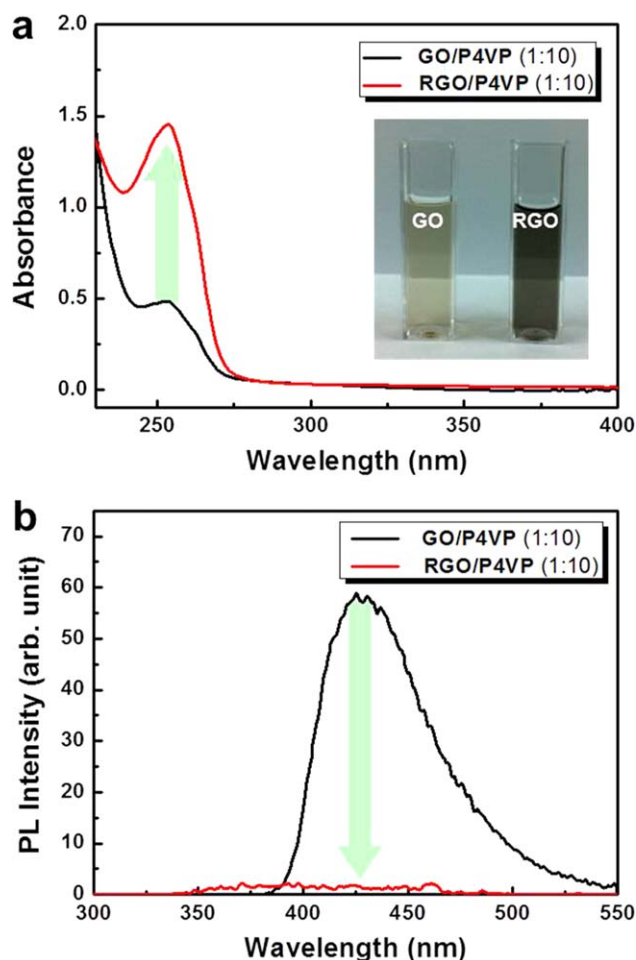


**Figure 2.** (a) UV-Vis and (b) PL spectra of both GO/P4VP mixture and RGO/P4VP assembly solutions (the insets are photos of both solutions). [Color figure can be viewed in the online issue, which is available at [wileyonlinelibrary.com](http://wileyonlinelibrary.com).]

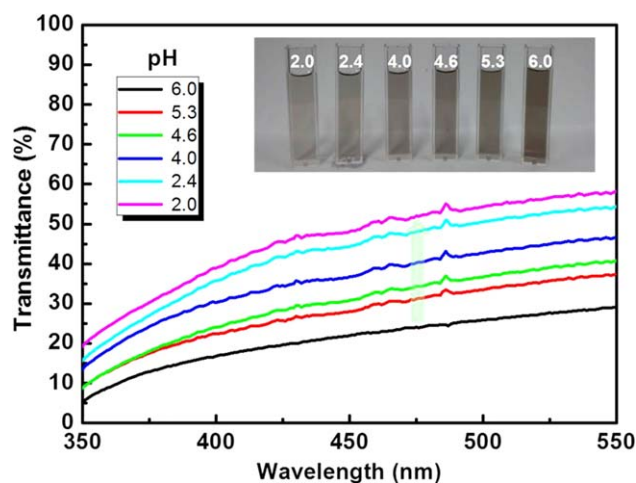


**Figure 3.** UV-Vis spectra of RGO/P4VP assembly solutions at different pH (the insets are photos of assembly solution at each pH). [Color figure can be viewed in the online issue, which is available at [wileyonlinelibrary.com](http://wileyonlinelibrary.com).]

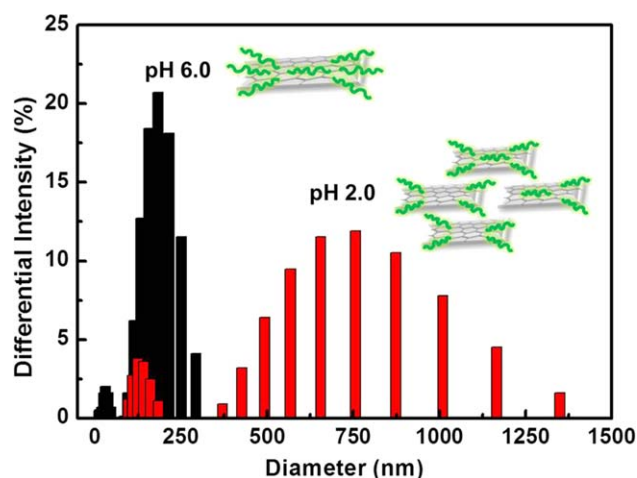


**Figure 4.** DLS data for RGO/P4VP assembly solution both at pH 2.0 and 6 (the insets are schematic illustration for the corresponding region). [Color figure can be viewed in the online issue, which is available at [wileyonlinelibrary.com](http://wileyonlinelibrary.com).]

because P4VP is readily soluble only in acidic condition. To prepare RGO/P4VP assembly, acidic P4VP solution was mixed with fresh GO solution (weight ratio of P4VP to GO is 10 : 1 or 100 : 1). Chemical reduction of GO/P4VP mixture by hydrazine at 80°C produced black-colored solution with no visible precipitation. Increased optical absorbance over all wavelengths in UV-Vis spectroscopy supports that recovery of  $\pi$ -conjugation is successfully accomplished in RGO/P4VP assembly [Figure 2(a)]. Complete disappearance of weak PL peak of GO at 426 nm after chemical reduction confirms that the formation of metallic RGO structure having zero band-gap from insulating or semiconducting GO having certain band gap is almost completed [Figure 2(b)]. To investigate the role of P4VP during the assembly formation, reduction of GO solution was performed in the absence of P4VP, producing insoluble black-colored graphite-like precipitation which is not soluble again in deionized water even with the addition of excess P4VP. These confirm that noncovalent anchoring of P4VP chains on RGO plate is effective and strong in RGO/P4VP assembly. Considering the process of chemical reduction of GO in the presence of P4VP, it is evident that as-formed RGO thermodynamically favors  $\pi$ - $\pi$  stacking of neighboring RGO plates, resulting in “graphite-like” structure as shown in Figure 3(a). But the presence of lots of P4VP chains in the medium hampers thermodynamically favorable stacking of RGO plates. Instead of  $\pi$ - $\pi$  stacking between neighboring RGO plates, RGO plate will statistically encounter  $\sigma$ -rich P4VP chains and might formulate RGO/P4VP assembly through  $\sigma$ - $\pi$  interaction. Therefore, it is believed that formation of RGO/P4VP assembly is favored under kinetic control while spontaneous stacking of neighboring RGO plates might be favored under thermodynamic control because  $\pi$ - $\pi$  interaction between RGO plates is typically much stronger than  $\sigma$ - $\pi$  interaction between molecules (Figure 1).<sup>28</sup>

#### Optical Modulation of RGO/P4VP Assembly

As-prepared RGO/P4VP assembly solution showed pH of 6.0 after complete reduction. Then, optical transmittance of RGO/P4VP assembly solution was measured at different pH.

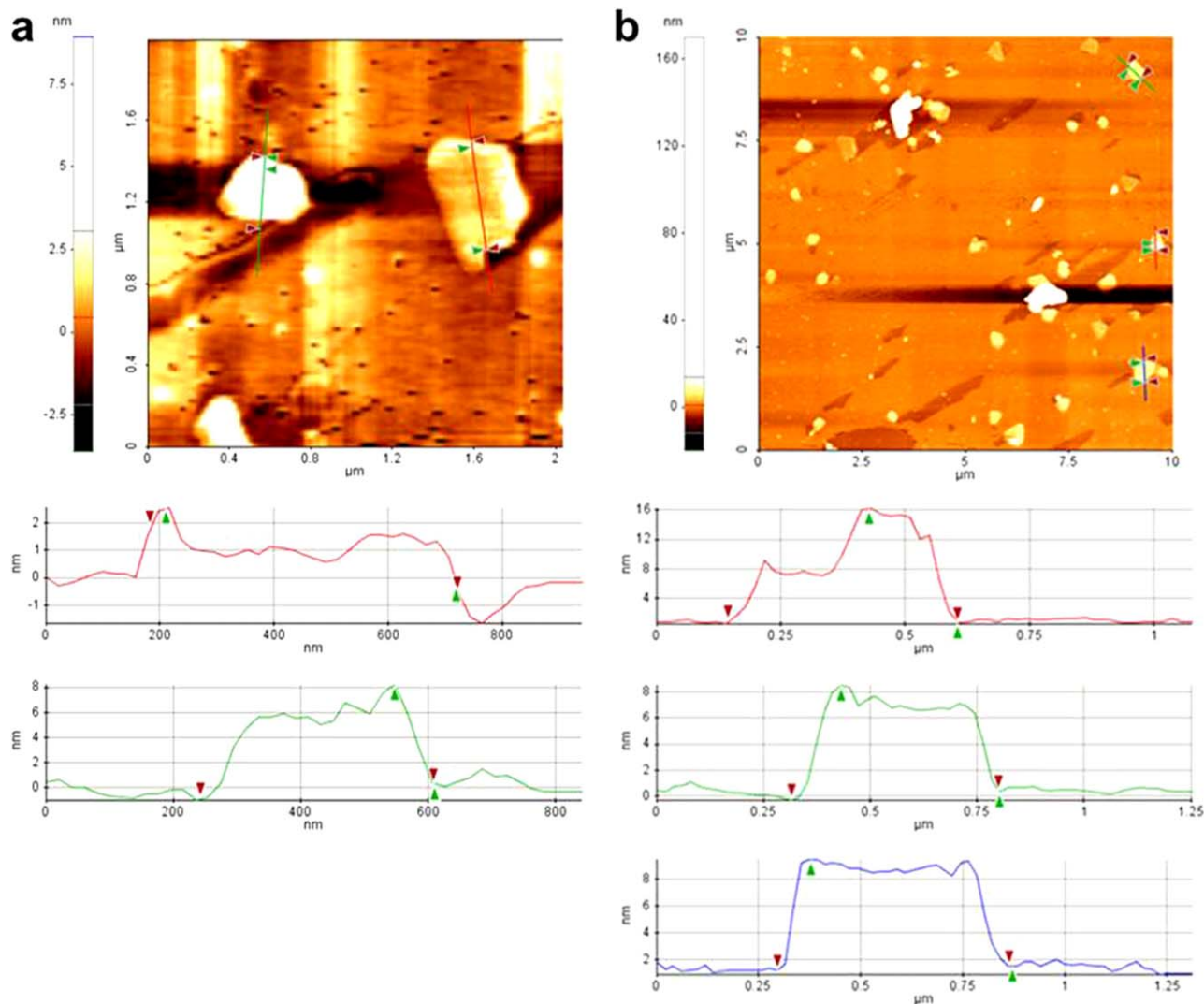


**Figure 5.** AFM images of RGO/P4VP assembly at pH of (a) 6.0 and (b) 2.0 (the bottom profiles are heights profiles for the colored lines in AFM images). [Color figure can be viewed in the online issue, which is available at [wileyonlinelibrary.com](http://wileyonlinelibrary.com).]

Concentration of RGO was set to be constant in all cases. While pH of RGO/P4VP assembly solution decreases, increase of optical transmittance was observed. Almost 2-fold increase of transmittance values at overall wavelength was observed in assembly solution at pH 2 compared with original optical transmittance of assembly solution at pH 6 as shown in Figure 3. This optical modulation of RGO/P4VP assembly is fully reversible by pH variation. This increase of optical transmittance of RGO/P4VP assembly at pH 2 might originate from the partial aggregation of assemblies at low pH. DLS analysis of RGO/P4VP assembly solution at pH 2 showed the formation of much bigger aggregates with average particle diameter of 750 nm compared with average particle diameter of RGO/P4VP assembly with 220 nm at pH 6 as shown in Figure 4. AFM image of RGO/P4VP assembly at pH 6 showed several graphene plates with thickness between 2 and 6 nm as shown in Figure 5(a). Increased plate thickness compared with the thickness of original GO (around 1 nm) confirms that P4VP chains are actually anchored on

RGO plates. At pH 2, bigger aggregates with thickness of more than 10 nm were monitored as shown in Figure 5(b). Therefore, it is regarded that RGP/P4VP assemblies are well separated each other at pH 6, resulting in much enhanced optical absorption of separated RGO plates. At pH 2, self-aggregation of several RGO/P4VP assemblies occurs, resulting in bigger and thicker structures having less optical absorption. This aggregation–disaggregation behavior of RGO/P4VP assembly at different pH might originate from the morphological variation of RGP/P4VP assembly. Because van der Waals interaction is independent of pH, another molecular interaction might contribute to above aggregation behavior. The presence of lots of pyridinium groups at pH 2 [below  $pK_a$  (3.4) of pyridine] will induce electrostatic repulsion between noncovalent interaction P4VP chains on RGO plate.<sup>29</sup> If this repulsion is stronger than  $\sigma$ – $\pi$  interaction between P4VP chains and RGP plate, detachment of P4VP chains from RGO plate might occur. This detachment of P4VP ligand can induce aggregation of neighboring RGO plates

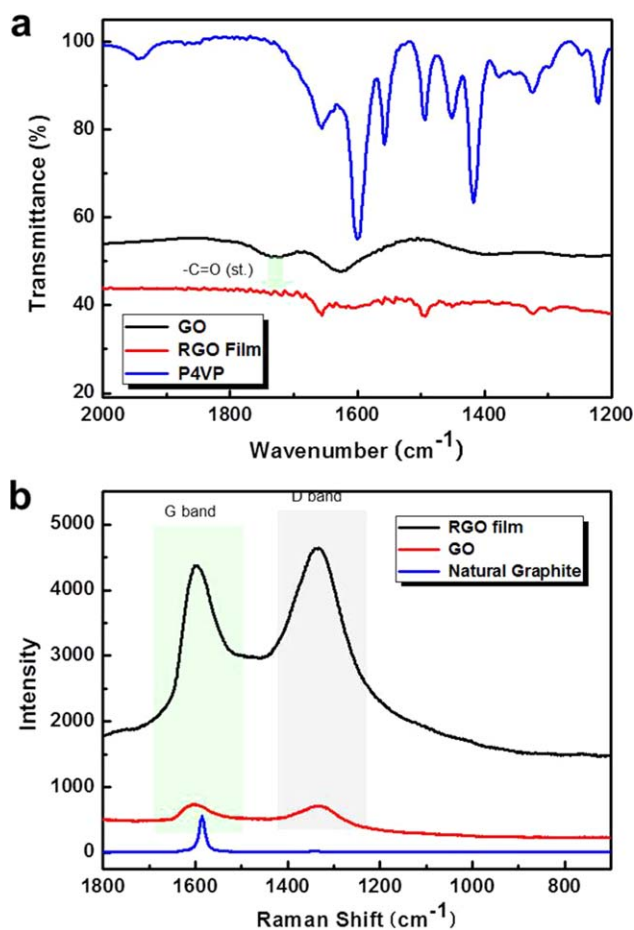


**Figure 6.** (a) FT-IR and (b) Raman spectra of GO, P4VP (or natural graphite), and RGO film. [Color figure can be viewed in the online issue, which is available at [wileyonlinelibrary.com](http://wileyonlinelibrary.com).]

having remaining P4VP chains. At pH 6, electrostatic repulsion is vanishing because deprotonation of pyridine rings occurs at pH higher than pK<sub>a</sub> of P4VP. Then, aggregated structures might disaggregate as individual P4VP/RGO assembly. All these results support that noncovalent interaction between RGO plates and P4VP chains can be intentionally engineered and therefore, much complex assembly structure can be formulated through noncovalent chemistry rather than covalent chemistry. Meanwhile, RGO/P4VP assembly is insoluble above pH 8 because the insolubility of P4VP in basic condition.

#### FT-IR and Raman Study

Both FT-IR and Raman analysis provide detailed structural information on RGO/P4VP assembly. Solution of RGO/P4VP assembly was vacuum filtered on anodizing aluminum oxide (AAO) membrane with pore size of 0.2 μm, resulting in RGO film with thickness of 100 nm. FT-IR spectra of filtered RGO film showed no presence of P4VP chains as shown in Figure 6(a). The reason why noncovalently anchored P4VP chains are detaching from RGO plate during filtration process is not clear. Therefore, it can be estimated that *s-p* interaction between P4VP chains and RGO plate vanishes and *p-p* interaction between RGO plates dominates during filtration process of

assembly solution. Carbonyl stretching (1730 cm<sup>-1</sup>) from carboxylic acid groups of GO was completely disappeared in RGO film, showing that chemical reduction to RGO is almost completed in the presence of P4VP. Raman spectra of prepared RGO film showed characteristic both D and G bands of RGO at 1335 and 1598 cm<sup>-1</sup>, respectively, as shown in Figure 6(b). The presence of D band which is not observed in the case of natural graphite supports that plate size of both GO and RGO is much smaller than natural graphite. The increased D to G band intensity ratio [I(D)/I(G)] of prepared RGO film compared with GO also well correlates with the other reports in the literature, confirming that chemical reduction to RGO is completed in the presence of P4VP.<sup>30</sup>

#### CONCLUSIONS

In summary, pH-responsive RGO/P4VP assembly was formulated and used to obtain the detailed information on the anchoring parameter and morphological features of RGO/polymer assembly through noncovalent approach. Control of pH triggers the change of morphology of RGO/P4VP assemblies in solution. It seems that dispersion state of RGO/polymer assembly depends on the effectiveness of noncovalent interaction between RGO plates and polymer chains. In strongly acidic medium, RGO/P4VP assembly aggregates each other, resulting less optical absorption. In weakly acidic medium, RGO/P4VP assemblies are well dispersed, resulting in increased optical absorption. This aggregation/deaggregation behavior of RGO/P4VP assembly on pH variation might be interesting for several applications such as pH sensor, targeted drug delivery, removable nanocatalyst, etc.

#### ACKNOWLEDGMENTS

This research was supported by Basic Science Research Program through the National Research Foundation of Korea (NRF) funded by the Ministry of Education, Science and Technology (2012-0004806), and this work was supported by Grant No.10041221 (Fundamental R&D Program for Core Technology of Materials funded) and Grant No. R0001826, and by Fusion Research R&D program (2012) from the Ministry of Trade, Industry & Energy (MOTIE), Republic of Korea. Mi Yeon Lee and Su Hyun Nam contributed equally to this project and should be considered co-first authors.

#### REFERENCES

- Noorden, R. V. *Nature* **2011**, *469*, 14.
- Liu, D.; Tanga, J.; Gooding, J. J. *J. Mater. Chem.* **2012**, *22*, 12435.
- Becerril, H. A.; Mao, J.; Liu, Z.; Stoltenberg, R. M.; Bao, Z.; Chen, Y. *ACS Nano* **2008**, *2*, 463.
- Stankovich, S.; Dikin, D. A.; Dommett, G. H. B.; Kohlhaas, K. M.; Zimney, E. J.; Stack, E. A.; Piner, R. D.; Nguyen, S. T.; Ruoff, R. S. *Nature* **2006**, *442*, 282.
- Kim, K. S.; Zhao, Y.; Jang, H.; Lee, S. Y.; Kim, J. M.; Kim, K. S.; Ahn, J. H.; Kim, P.; Choi, J. Y.; Hong, B. H. *Nature* **2009**, *457*, 706.

6. Georgakilas, V.; Otyepka, M.; Bourlinos, A. B.; Chandra, V.; Kim, N.; Kemp, K. C.; Hobza, P.; Zboril, R.; Kim, K. S. *Chem. Rev.* **2012**, *112*, 6156.
7. Fan, X.; Peng, W.; Li, Y.; Li, X.; Wang, S.; Zhang, G.; Zhang, F. *Adv. Mater.* **2008**, *20*, 4490.
8. Li, D.; Müller, M. B.; Gilje, S.; Kaner, R. B.; Wallace, G. G. *Nat. Nanotech.* **2008**, *3*, 101.
9. Shan, C.; Yang, H.; Han, D.; Zhang, Q.; Ivaska, A.; Niu, L. *Langmuir* **2009**, *25*, 12030.
10. Salavagione, H. J.; Gómez, M. A.; Martínez, G. *Macromolecules* **2009**, *42*, 6331.
11. Sahoo, S.; Bhattacharya, P.; Hatui, G.; Ghosh, D.; Das, C. K. *J. Appl. Polym. Sci.* **2013**, DOI:10.1002/APP.38285.
12. Xu, Y.; Bai, H.; Lu, G.; Li, C.; Shi, G. *J. Am. Chem. Soc.* **2008**, *130*, 5856.
13. Yang, H.; Zhang, Q.; Shan, C.; Li, F.; Han, D.; Niu, L. *Langmuir* **2010**, *26*, 6708.
14. Yoon, S. In, I. *Chem. Lett.* **2010**, *39*, 1160.
15. Yoon, S.; In, I. *J. Mater. Sci.* **2011**, *46*, 1316.
16. Lee, D. Y.; Yoon, S.; Oh, Y. J.; Park, S. Y.; In, I. *Macromol. Chem. Phys.* **2011**, *212*, 336.
17. Lee, D. Y.; Khatun, Z.; Lee, J.-H.; Lee, Y.-K.; In, I. *Biomacromolecules* **2011**, *12*, 336.
18. Lee, J. Y.; In, I. *Chem. Lett.* **2012**, *41*, 127.
19. Yeo, M. Y.; Park, S. Y.; In, I. *Chem. Lett.* **2012**, *41*, 197.
20. Ko, T. Y.; Kim, S. Y.; Kim, H. G.; Moon, G.-S.; In, I. *Chem. Lett.* **2013**, *42*, 66.
21. Jeong, G.; Kim, H. G.; Nam, J. A.; Park, S. Y.; In, I. *Chem. Lett.* **2013**, *42*, 200.
22. Lee, M. Y.; Kim, S. Y.; Kim, H. G.; In, I. *Chem. Lett.* **2013**, *42*, 48.
23. Haugh, E. F.; Hirschfelder, J. O. *J. Chem. Phys.* **1955**, *23*, 1778.
24. Qin, W.; Li, X.; Bian, W. W.; Fan, X. J.; Qi, J. Y. *Biomaterials* **2010**, *31*, 1007.
25. Gburski, Z.; Górny, K.; Raczynski, P.; Dawid, A. Impact of the Carbon Allotropes on Cholesterol Domain: MD Simulation, Carbon Nanotubes - Growth and Applications; InTech (Available from: <http://www.intechopen.com/books/carbon-nanotubes-growth-and-applications/impact-of-the-carbon-allotropes-on-cholesterol-domain-md-simulation>).
26. Ren, L.; Liu, T.; Guo, J.; Guo, S.; Wang, X.; Wang, W. *Nanotechnology* **2010**, *21*, 335701.
27. Marcano, D. C.; Kosynkin, D. V.; Berlin, J. B.; Sinitskii, A.; Sun, Z.; Slesarev, A.; Alemany, L. B.; Lu, W.; Tour, J. M. *ACS Nano* **2010**, *4*, 4806.
28. Nic, M.; Jirat, J.; Kosata, B., eds. (2006–). “Van der Waals forces”. IUPAC Compendium of Chemical Terminology (Online ed.). DOI:10.1351/goldbook.V06597.
29. Fujii, S.; Read, E. S.; Binks, B. P.; Armes, S. P. *Adv. Mater.* **2005**, *17*, 1014.
30. Kudin, K. N.; Ozbas, B.; Schniepp, H. C.; Prud'homme, R. K.; Aksay, I. A.; Car, R. *Nano Lett.* **2008**, *8*, 36.